RSC Advances

ROYAL SOCIETY OF CHEMISTRY

www.rsc.org/advances

Fabrication of Intelligent Poly(N-isopropylacrylamide) / Silver Nanoparticles Composite Films with Dynamic Surface-Enhanced Raman Scattering Effect

Lin Wang,[a] Xiaomei Zhao,[a] Yan Zhang,[a] Wenqi Zhang,[a] Tianrui Ren,[a] Zhihong Chen,[b] Feng Wang*[a] and Haifeng Yang*[a]

a The Education Ministry Key Lab of Resource Chemistry, Shanghai Key Laboratory of Rare Earth Functional Materials, Shanghai Municipal Education Committee Key Laboratory of Molecular Imaging Probes and Sensors, and Department of Chemistry, Shanghai Normal University, Shanghai, 200234, P. R. China.

b College of Information, Mechanical and Electrical engineering, Shanghai Normal University, Shanghai, 200234, P. R. China.

Abstract

Intelligent PNIPAAm / AgNPs composite film was fabricated by the simple assembly of silver nanoparticles on the surface of photo-polymerized PNIPAAm film via electrostatic interaction. Surface enhanced Raman scattering study and finite-difference time-domain simulation demonstrated that the local electric field intensity and the SERS intensity of this resultant composite film can be easily tuned by changing the interparticle distance triggered with temperature or solvent variations. The composite film showed a high stability in polar organic solvent and concentrated saline solution. As a perspective, the smart composite film might find its applications as a SERS sensor for temperature / solvent variation detection as well as a versatile SERS substrate for the detection of analyte in sea water and organic solvent.

1 Introduction

In comparison with other metal nanoparticles, silver nanoparticles (AgNPs) have attracted considerable attention because of their dominant plasmonic optical properties and have been applied in many fields such as sensing, photocatalysis, biomedical imaging, *etc*.[1–5] One of the most intriguing optical properties of AgNPs is localized surface plasmon resonance (LSPR), which is the collective oscillation of the conduction-band electrons induced by the interacting electromagnetic field.[6] The enhanced electromagnetic field at the surface of AgNPs can significantly amplify the Raman signal of the surrounding analyte, which is the basis of their application as surface enhanced Raman scattering (SERS) substrate.[7] Further studies showed that nanostructures and gaps less than 10 nm (also termed "hot-spots") can exponentially enhance the SERS signal, which has been applied as a sensitive and powerful analytical technique for the ultrasensitive detection of molecules.[8–10] Various methods have been developed to introduce hot-spots on SERS substrates via either top-down[11, 12] or bottom-up[13–15] approach. However, in most cases, once the SERS substrates are formed, the spatial distribution of AgNPs is fixed.[14, 16] Therefore, the number of hot-spots and the enhancement factor of the substrate are also fixed and cannot respond to environmental stimuli. On the contrary, the dynamic SERS substrates with variable interparticle distances can not only enhance SERS signals by external stimuli but also monitor environmental variations such as temperature, pH, and solvent *etc.*, making them suitable for environmental changes detection. For example, temperature tunable SERS nanosensers could act as temperature probes of biological systems *in vivo*.[17]

Intelligent polymers (also called smart polymer) that can reversibly change their properties in response to environmental stimuli, have drawn numerous research interests in the preparation of

dynamic SERS substrates.[18-22] Among them, poly(N-isopropylacrylamide) (PNIPAAm) has been studied in detail with regard to its well-known phase behavior in aqueous solutions, which undergoes a reversible phase transition at its lower critical solution temperature (LCST, ~ 32 ^{o}C in water). The conformation of PNIPAAm chain changes from a swollen state (below LCST) to a shrunken state (above LCST) upon temperature increments due to the weakened amide - water interaction and the enhanced hydrophobic interaction between isopropyl groups.[23, 24] The conformational changes together with the significant dimensional variations make PNIPAAm a good candidate for the preparation of dynamic SERS substrates.[25–29] However, many of the reported dynamic SERS substrates are prepared tortuously or are time consuming. In addition, AgNPs fabricated by *in situ* silver ion reduction in some dynamic SERS substrates are hard to control in terms of size and particle number. What's more, the conformational changes of PNIPAAm can also be triggered by solvent changes or salt ion, yet up to now few reports can be found about the responses of dynamic SERS substrate to such stimuli.

We report in this work a facile approach to fabricate PNIPAAm / AgNPs composite films, in which uniform silver nanoparticles were densely loaded on photo-polymerized PNIPAAm film via electrostatic interaction. The temperature-dependent optical properties of the composite film were confirmed by UV-reflectance spectroscopy and Finite-Difference Time-Domain (FDTD) simulation. When the PNIPAAm / AgNPs composite film was used as dynamic SERS substrates for detecting 4-mercaptopyridine in an aqueous solution, the SERS signals could be modulated by temperature and solvent changes and are relatively stable even at high salt concentrations. Therefore, the composite film holds promise as a SERS sensor for temperature detection, and can also act as a versatile SERS substrate for analyte detection in sea water and many organic

solvents.

2 Experimental Section

2.1 Materials

N-isopropylacrylamide (NIPAAm, 98%, Aladdin), N,N'-methylene bisacrylamide (MBA, 97%, Aladdin), 2-[4-(2-hydroxy-2-methyl-1-oxopropyl)phenoxy]ethyl ester (I2959, TCI) , 4-mercaptopyridine (4-Mpy, TCI), 2-aminoethyl methacrylate hydrochloride (AEMH, 98%, HWRK Chem), anthracene (HWRK Chem), methanol (AR, Sinopharm Chemistry Reagent Co), ethanol(AR, Sinopharm Chemistry Reagent Co), silver nitrate ($AgNO_3$, AR, Sinopharm Chemistry Reagent Co), crystal violet (AR, Sinopharm Chemistry Reagent Co), tri-sodium citrate (AR, Sinopharm Chemistry Reagent Co) and sodium chloride (NaCl, AR, Sinopharm Chemistry Reagent Co) were used as received. All deionized water used in the synthesis and characterization was acquired by UPH series of tap water ultrapure water machine.

2.2 Synthesis of PNIPAAm film

PNIPAAm films were synthesized by photopolymerization.[30] In a typical procedure, 0.90 g NIPAAm , 0.01 g MBA (crosslinking agent), 0.05 g I2959 (photoinitiator) and 0.09 g 2-aminoethyl methacrylate hydrochloride (functional monomer) were dissolved in 1mL methanol. Then one drop (about 80 μL) of such solution was spread on a polytetrafluoroethylene (PTEF) petri dish and left untouched for 10 min under ambient conditions to allow the solution to reach saturation after solvent evaporation. The solution droplet was then covered with a cover glass and exposed to UV radiation (365 nm or 264 nm) for 15 min. The cover glass was removed and the crosslinked film was peeled off from the PTFE dish and washed in cold water for 3 times to get the PNIPAAm film.

2.3 Synthesis of AgNPs suspension

AgNPs were synthesized according to the method reported by Lee and Meisel.[31] 0.001 M silver nitrate was dissolved in 150 mL deionized water. After the solution was heated to boiling, 3 mL of 1% tri-sodium citrate solution was added slowly under vigorous stirring. The reaction was kept for 6 h under boiling temperature to obtain the product Ag colloid with desired sizes. A due amount of Milli-Q water was added to obtain 125 mL of Ag colloid (the final concentration of Ag was 1.2 mM).

2.4 Preparation of PNIPAAm / AgNPs composite film

PNIPAAm film was immersed in 3 mL AgNPs suspension for 1 h. After that, the film was taken out and washed in deionized water for three times to get the clean PNIPAAm / AgNPs composite film.

2.5 Finite-Difference Time-Domain Simulation

The FDTD method was employed to simulate the electric field intensities and distributions at the surface of the SERS substrate by FDTD Solution software. The incident light is defined as a plane wave with an injection direction that is parallel to Z axis. For room temperature simulation, the calculation region was $100\times60\times60$ nm^3, for high temperature simulation the region was set at $78\times60\times60$ nm^3. In both cases the boundary conditions were set to periodic for X and Y and perfecting matched layer (PML) for Z. A mesh override region was set to 0.25 nm around the nanoparticles. The overall simulation time was set to 1000 fs. A 2D Z-normal frequency domain profile monitor with z=0 was applied to measure the electric field profile of the SERS substrate at the wavelength of 633 nm.

2.6 Characterization and Measurement

UV-vis spectrum of Ag colloid was collected using a Model 760-CRT double-beam spectrophotometer (Shanghai Precision and Scientific Instrument Co.,Ltd.). UV-reflectance spectra of AgNPs / PNIPAAm at 25 ^{o}C and 40 ^{o}C were collected using a UH4150 UV/visible/near infrared spectrophotometer (Hitachi Co.,Ltd). TEM images of AgNPs were acquired on a Model JEM-2100EXII transmission electron microscope (JEOL Co., Ltd.), operating at 200 kV. Fourier transform infrared spectra (FT－IR) were collected using a Nicolet infrared spectrometer (AVATAR-370-FTIR). The zeta potential was measured using a Malvern Zetasizer Nano ZS model ZEN3600 (Worcestershire, U.K.) equipped with a standard 633-nm laser. SERS spectra were recorded using a Jobin Yvon confocal laser Raman system (SuperLabRam II), which was equipped with a He–Ne laser at 632.8 nm with a power of ca. 5 mW. Each spectrum was obtained by three accumulations and the acquisition time was set at10 sec.

3 Result and Discussion

A three-step approach was employed for the fabrication of PNIPAAm / AgNPs composite film, as shown in Scheme1. The detail fabrication is presented in the experimental section. In the first step, PNIPAAm film with amine groups was synthesized by photopolymerization.[30] Raman spectra of NIPAAm before and after UV radiation are shown in Figure 1A. Three peaks related to C=C double bond at 1247, 1405 and 1620 cm^{-1} could be clearly seen in Figure 1A(a). After UV irradiation for 15 min these three peaks dramatically decreased (Figure 1A(b)), which confirmed the transition of monomer into polymers.[32] FTIR was also utilized to monitor the photopolymerization (Figure1B). The peaks at 1414 and 1624 cm^{-1} respectively due to C=C and -C=C stretching vibrations in NIPAAm monomer disappeared after UV irradiation, which is consistent with the results of Raman study. What's more, after thoroughly rinsing with cold water

to remove unreacted monomers, the absorption peak at 3450 cm^{-1} in FTIR spectrum of PNIPAAm (N – H vibration in AEMH segment) can be clearly seen,[33] confirming the incorporation of amine group in the PNIPAAm chain.

In the second step, positively charged AgNPs were prepared according to Lee and Meisel's protocol. Uniform AgNPs with an average diameter of 35±4 nm were obtained (Figure 2A). This kind of AgNPs suspension showed an absorption peak at 407 nm in UV-vis spectrum (Figure 2B), which agrees with the previous report.[34, 35] This citrate protected AgNPs showed a negative charge (- 34.7 ± 2 mV) by zeta-potential measurement, which will facilitate the further assembly of AgNPs on amine-group bearing PNIPAAm film.

In the third step, PNIPAAm / AgNPs composite film was fabricated by electrostatic assembly of AgNPs on amine-group bearing PNIPAAm film. The color of the translucent PNIPAAm film gradually became dark brown (Figure S1a, b) after immersing the film in AgNPs suspension for 1 h (Figure S2). After rinsing the film with water and drying it in the air, a greyish-green luster was observed (Figure S1c). SEM image (Figure 3A) also showed a closely stacked AgNPs layer, indicating the successful assembly of AgNPs on PNIPAAm film.

As PNIPAAm / AgNPs composite film is opaque, UV-reflectance spectroscopy was performed to study the thermo-sensitivity of the film at 25 ^{o}C and 40 ^{o}C. Figure 3B showed that the reflectivity of the composite film at 40 ^{o}C was larger than that at 25 ^{o}C over a wide wavelength ranges (300 ~ 700 nm). This could be explained by the closeness of the AgNPs induced by the shrinking of PNIPAAm chain network upon heating.[36, 37, 38] With closeness of the AgNPs and the increase of the particle density, the extinction / anti-reflection feature of the AgNPs weakened, the composite film then becomes similar to the reflective bulk silver film at higher temperatures.

The calculation of interparticale distances between the adsorbed AgNPs at low and high temperatures was performed in order to better understand the dynamic changes of the PNIPAAm /AgNPs composite film. Based on the assumption that all AgNPs were distributed evenly on the PNIPAAm film with a pattern schemed in Figure S3, we can calculate the average interparticle distance between the AgNPs at 25 ^{o}C and 40 ^{o}C. Specifically, the density of AgNPs in dry state was obtained from SEM image (Figure 3A), and dimensional variations of the PNIPAAm / AgNPs composite film can be evaluated from digital camera image (DCI) (Figure S1) at 25 ^{o}C, 40 ^{o}C and dry state. According to calculation results, the interparticle distance decreased from 15 nm at 25 ^{o}C to 4 nm at 40 ^{o}C, indicating the shrinking of PNIPAAm chain at higher temperatures and the increased particle density of the composite film. The observation further corroborates the UV-reflectance result. As a consequence, the PNIPAAm / AgNPs composite film can be expected to serve as a dynamic SERS substrate.

To further understand the mechanism of the SERS effect tuned by temperature, the near-field electric distribution of the PNIPAAm / AgNPs composite film was calculated based on FDTD solution software. A thin layer of water (Z = 0 ~ 30 nm) and PNIPAAm (Z = -30 ~ 0 nm) was added to mimic the real condition. The refractive index of PNIPAAm was set to be 1.35 at 25 ^{o}C and 1.65 at 40 ^{o}C.[39] As shown in Figure 4, the simulated electric field profiles at different temperatures showed a significant field enhancement at 40 ^{o}C than at 25 ^{o}C. The thermo-induced local electric field enhancement depicted that the PNIPAAm / AgNPs composite film with high sensitivity could be employed as the dynamic SERS substrates for molecular sensing.

Using 4-mercaptopyridine (4-Mpy) as a probe molecule due to its distinctive Raman spectral feature and strong binding with AgNPs via S-Ag bond,[40-42] the SERS activities of PNIPAAm /

AgNPs composite film with increasing temperature were investigated. The recorded SERS spectra are presented in Figure 5A. The bands at 1006 and 1097 cm^{-1} can be assigned to the ring breathing and C-C-C/C-S stretching, respectively. A peak at 1216 cm^{-1} is assigned to the β(CH)/ β (NH) stretching. The peaks at 1577 and 1609 cm^{-1} are from the ring stretch modes of the 4-Mpy molecules with deprotonate and protonated nitrogen atoms. The occurrence of Raman band at 1097 cm^{-1} corresponding to the ring breathing / C-S stretching mode indicates that 4-Mpy was bound to the AgNPs surface through the sulfur atom.[35, 42, 43] Figure 5B shows the temperature-dependent SERS intensity at 1097 cm^{-1}, which increased sharply at ~ 35 ^{o}C and then leveled off with temperature increasing. It's not surprising to find that phase transition of PNIPAAm (LCST ~32 ^{o}C) just happened in the temperature region (30-35 ^{o}C) where the SERS signal showed a significant improvement of at least 3 fold. Moreover, upon cooling from 40 ^{o}C to 25 ^{o}C, the intensity could go back to the original intensity at 25^{o}C. As seen in Figure 6, showing the reversible thermo-induced change can be repeated for at least three-times. Therefore, the thermo-induced SERS signal changes on the PNIPAAm / AgNPs composite film is quite reversible. Similar results were obtained while detecting CV (10^{-9} M) and anthracene (10^{-4} M) on the composite film (Figure S3 and Figure S4). A clear increase in SERS intensity can be observed with temperature increases. These results indicate that the PNIPAAm / AgNPs composite film hold potential as a SERS sensor for temperature variation detection.

In addition, the reproducibility of the PNIPAAm / AgNPs composite film was investigated by comparing SERS signals from 20 different spots on the same composite film (Figure 7A) and different composite films (Figure 7C). The peak at 1097 cm^{-1} was chosen to evaluate the reproducibility of composite film (Figure 7B and Figure 7D). The relative standard deviations are

17.5 % (Figure 7B) for spot-to-spot and 18.6 % (Figure 7D) for batch-to-batch respectively, which prove that the SERS substrate exhibits a good reproducibility.

PNIPAAm/AgNPs composite film was immersed in basic, acid or salt solution to study the durability of the film. The SERS intensity is relatively stable within pH range of 5~9, but significantly decreases at lower pH value ($\leqslant$4) or higher pH value ($\geqslant$10) (Figure S6). As above mentioned, the main driving force of the formation of PNIPAAm/AgNPs composite film is electrostatic interaction, harsh pH conditions might destabilize the electrostatic interaction between PNIPAAm chain and AgNPs, leading to the detachment of AgNPs from the film and the decreased SERS signal. Interestingly, the SERS signal is reasonably stable even at high salt concentration equal to 15 w% (Figure S7). This might be attributed to the "salting out" effect of PNIPAAm chains: the chains dehydrate and collapse at lower temperature with the presence of salt ions,[44] protecting the AgNPs against detachment from the film.

As PNIPAAm chain can also respond to other stimuli such as solvent polarity change, SERS intensities of 4-Mpy in H_2O, EtOH and H_2O / EtOH mixture were studied. Figure 8c shows a significant SERS signal increase in H_2O / EtOH mixture with a volume ratio of 1:1 compared to that in pure H_2O and pure EtOH (Figure 8a and Figure 8b). Though the introduction of organic solvent can alter the LSPR of AgNPs,[45] the SERS signal normally becomes weaker in organic solvent (herein, EtOH) than in water (Figure 8b).[46] Generally the SERS enhancement factor in nonaqueous media is only 1/10 to 1/100 of that in aqueous media.[47] So the highest SERS signal of PNIPAAm / AgNPs composite film in H_2O/EtOH mixture in this study could only be attributed to the greatest enhancement of LSPR induced by the closeness of AgNPs in solvent mixture such as 1:1 v/v H_2O / EtOH. As well known, the competition of ethanol with water will cause the

dehydration and the collapse of PNIPAAm chain, leading to the shrinking of PNIPAAm film and the decreased interparticle distances. [48, 49] This finally caused the formation of more SERS hot-spots in 1:1 v/v H_2O / EtOH mixture. In Figure 8c, it's worth mentioning that SERS signals related to ring-breathing mode at 1006 cm^{-1} , β(CH)/ β (NH) stretching mode at 1216 cm^{-1} and the ν(C-C) with protonated nitrogen mode at 1609 cm^{-1} become much stronger compared to that of the ν(C-C) with deprotonated nitrogen mode at 1577 cm^{-1}, also hinting the improved charge transfer process and the formation of hydrogen bond between the N atom of 4-Mpy and the hydroxyl group of ethanol.

To evaluate the long-term stability of the PNIPAAm / AgNPs composite film as SERS substrate, the composite film was simply stored in water for 4 months. The composite film was then taken out and the SERS intensity of the analyte was measured. Figure S8 showed that the SERS signal of 4-Mpy only decreased 12.0 % compared to that of the original value, illustrating the good stability of the PNIPAAm / AgNPs composite film.

4 Conclusion

In summary, a smart PNIPAAm / AgNPs composite film was designed and fabricated by the simple assembly of negatively charged silver nanoparticles on photo-polymerized, amine group-bearing PNIPAAm film via electrostatic interaction. Interparticle distance changes among adjacent AgNPs on the composite film triggered by temperature or solvent variations can drastically alter the optical properties of the composite film. Eventually, SERS signals of the composite film could be modulated by temperature and solvent changes. The proposed dynamic SERS substrate even exhibited high durability under high salt condition. Therefore, this kind of

composite film can be expected to be utilized as a SERS sensor for temperature / solvent variation detection and for detecting analyte in sea water or in organic solvent.

Acknowledgements

The authors are grateful for the financial support provided by Shanghai Municipal Education Commission (Grant No. 13ZZ101 and Grant No. 14YZ072), Science and Technology Commission of Shanghai Municipality (Grant No. 14ZR1430200).

References:

1. X. Fan, W. Zheng and D. J. Singh, *Light: Science & Applications*, 2014, **3**, e179.
2. F. Lorestani, Z. Shahnavaz, P. Mn, Y. Alias and N. S. A. Manan, *Sensors and Actuators B: Chemical*, 2015, **208**, 389-398.
3. J. Wackerlig and P. A. Lieberzeit, *Sensors and Actuators B: Chemical*, 2015, **207**, 144-157.
4. M. Meena Kumari, J. Jacob and D. Philip, *Spectrochimica Acta Part A: Molecular and Biomolecular Spectroscopy*, 2015, **137**, 185-192.
5. H. Wang, X. Jiang, X. Wang, X. Wei, Y. Zhu, B. Sun, Y. Su, S. He and Y. He, A*nal. Chem.*, 2014, **86**, 7368-7376.
6. G. Marcelo and M. Fernández-García, *RSC Adv.*, 2014, **4**, 11740.
7. J. N. Anker, W. P. Hall, O. Lyandres, N. C. Shah, J. Zhao and R. P. Van Duyne, *Nat. Mater.*, 2008, **7**, 442-453.
8. A. Lee, G. F. S. Andrade, A. Ahmed, M. L. Souza, N. Coombs, E. Tumarkin, K. Liu, R. Gordon, A. G. Brolo and E. Kumacheva, *J. Am. Chem. Soc.*, 2011, **133**, 7563-7570.
9. D. Lim, K. Jeon, H. M. Kim, J. Nam and Y. D. Suh, *Nat. Mater.*, 2009, **9**, 60-67.
10. M. Moskovits, *Nature*, 2010, **464**, 357.
11. D. He, B. Hu, Q. Yao, K. Wang and S. Yu, *ACS Nano.*, 2009, **3**, 3993-4002.
12. C. Leiterer, D. Zopf, B. Seise, F. Jahn, K. Weber, J. Popp, D. Cialla-May and W. Fritzsche, *J. Nanopart. Res.*, 2014, **16**.
13. B. Yan, A. Thubagere, W. R. Premasiri, L. D. Ziegler, L. Dal Negro and B. M. Reinhard, *ACS Nano.*, 2009, **3**, 1190-1202.
14. A. Li, Z. Baird, S. Bag, D. Sarkar, A. Prabhath, T. Pradeep and R. G. Cooks, *Angewandte Chemie International Edition*, 2014, **53**, 12528-12531.
15. Z. Zuo, K. Zhu, L. Ning, G. Cui, J. Qu, Y. Cheng, J. Wang, Y. Shi, D. Xu and Y. Xin, *Appl. Surf. Sci.*, 2015, **325**, 45-51.
16. M. V. Cañamares, J. V. Garcia-Ramos, J. D. Gómez-Varga, C. Domingo and S. Sanchez-Cortes, *Langmuir*, 2005, **21**, 8546-8553.
17. J. Kneipp, H. Kneipp, B. Wittig and K. Kneipp, *Nano Lett.*, 2007, **7**, 2819-2823.
18. R. A. Álvarez-Puebla, R. Contreras-Cáceres, I. Pastoriza-Santos, J. Pérez-Juste and L. M. Liz-Marzán, *Angewandte Chemie International Edition*, 2009, **48**, 138-143.
19. D. Wu, Y. Sun, X. Xu, S. Cheng, X. Zhang and R. Zhuo, *Biomacromolecules*, 2008, **9**, 1155-1162.
20. T. Wu, Q. Zhang, J. Hu, G. Zhang and S. Liu, *Journal of Materials Chemistry*, 2012, **22**, 5155.
21. P. Yin, Y. Chen, L. Jiang, T. You, X. Lu, L. Guo and S. Yang, *Macromol. Rapid. Comm.*, 2011, **32**, 1000-1006.
22. A. C. Manikas, G. Romeo, A. Papa and P. A. Netti, *Langmuir*, 2014, **30**, 3869-3875.
23. J. Kim and T. R. Lee, *Langmuir*, 2007, **23**, 6504-6509.
24. G. Bokias, D. Hourdet, I. Iliopoulos, G. Staikos and R. Audebert, *Macromolecules*, 1997, **30**, 8293-8297.
25. Y. Wu, F. Zhou, L. Yang and J. Liu, *Chem. Commun.*, 2013, **49**, 5025.
26. H. Gehan, L. Fillaud, M. M. Chehimi, J. Aubard, A. Hohenau, N. Felidj and C. Mangeney, *ACS Nano.*, 2010, **4**, 6491-6500.

27. M. Mueller, M. Tebbe, D. V. Andreeva, M. Karg, R. A. Alvarez Puebla, N. Pazos Perez and A. Fery, *Langmuir*, 2012, **28**, 9168-9173.
28. X. Liu, C. Zhang, J. Yang, D. Lin, L. Zhang, X. Chen and L. Zha, *RSC Adv.*, 2013, **3**, 3384.
29. S. Ganta, H. Devalapally, A. Shahiwala and M. Amiji, *J. Control. Release.*, 2008, **126**, 187-204.
30. F. Wang, H. He, X. Wang, Z. Li, D. Gallego-Perez, J. Guan and L. J. Lee, *Anal. Chem.*, 2012, **84**, 9439-9445.
31. P. C. Lee and D. Meisel, *J. Phys. Chem.*, 1982, **86**, 3391-3395.
32. D. N. Rockwood, D. B. Chase, R. E. Akins and J. F. Rabolt, *Polymer*, 2008, **49**, 4025-4032.
33. X. Wang, Y. Chen, W. Zhou, Z. Huang, Z. Guo and Y. Hu, *J. Mater. Sci.*, 2009, **44**, 4710-4714.
34. B. Fei, Z. Xin-Zheng, W. Zhen-Hua, W. Qiang, H. Hao and X. Jing-Jun, *Chinese Phys. Lett.*, 2008, **25**, 4463-4465.
35. A. G. M. Da Silva, M. L. de Souza, T. S. Rodrigues, R. S. Alves, M. L. A. Temperini and P. H. C. Camargo, *Chemistry - A European Journal*, 2014, **20**, 15040-15046.
36. C. Zhang, K. Lv, H. Huang, H. Cong and S. Yu, *Nanoscale*, 2012, **4**, 5348-5355.
37. D. R. Willett and G. Chumanov, *Plasmonics*, 2014, **9**, 1391-1396.
38. X. M. Han, J. Q. Wang, S. Zhang, F. Y. Meng and T. Han, *Acta Phys. Sin.,* 2011, ***60***, 027303.
39. M. Toma, U. Jonas, A. Mateescu, W. Knoll and J. Dostalek, *The Journal of Physical Chemistry C*, 2013, **117**, 11705-11712.
40. L. Zhang, Y. Bai, Z. Shang, Y. Zhang and Y. Mo, *J. Raman Spectrosc.*, 2007, **38**, 1106-1111.
41. H. Guo, L. Ding and Y. Mo, *J. Mol. Struct.*, 2011, **991**, 103-107.
42. Y. Wang, Z. Yu, W. Ji, Y. Tanaka, H. Sui, B. Zhao and Y. Ozaki, *Angewandte Chemie International Edition*, 2014, **53**, 13866-13870.
43. Y. Wang, Z. Sun, H. Hu, S. Jing, B. Zhao, W. Xu, C. Zhao and J. R. Lombardi, *J RAMAN SPECTROSC*, 2007, **38**, 34-38.
44. Y. Zhang, S. Furyk, D. E. Bergbreiter and P. S. Cremer, *J. Am. Chem. Soc.*, 2005, **127**, 14505-14510.
45. S. Nath, S. Jana, M. Pradhan and T. Pal, *Journal of colloid and interface science,* 2010, ***341***, 333-52.
46. C. Pérez León, L. Kador, B. Peng and M. Thelakkat, *The Journal of Physical Chemistry B*, 2005, **109**, 5783-5789.
47. R. Gu, P. Cao and J. Yao, *Spectroscopy and Spectral analysis,* 1999, ***19***, 531-534.
48. M. C. Arndt and G. Sadowski, *Macromolecules*, 2012, **45**, 6686-6696.
49. I. Anac, A. Aulasevich, M. J. N. Junk, P. Jakubowicz, R. F. Roskamp, B. Menges, U. Jonas and W. Knoll, *Macromol. Chem. Phys.*, 2010, **211**, 1018-1025.

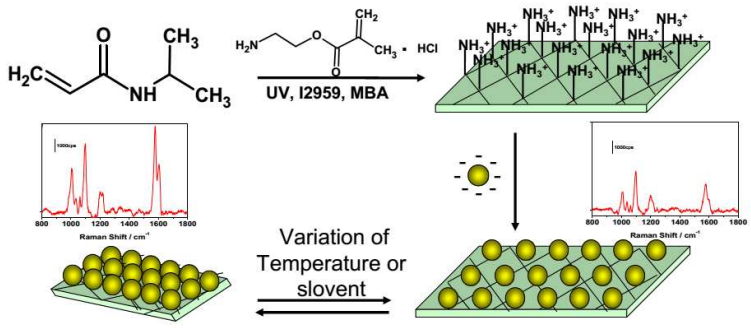

Scheme1. Shematic illustration of the fabrication of PNIPAAm / AgNPs composite film.

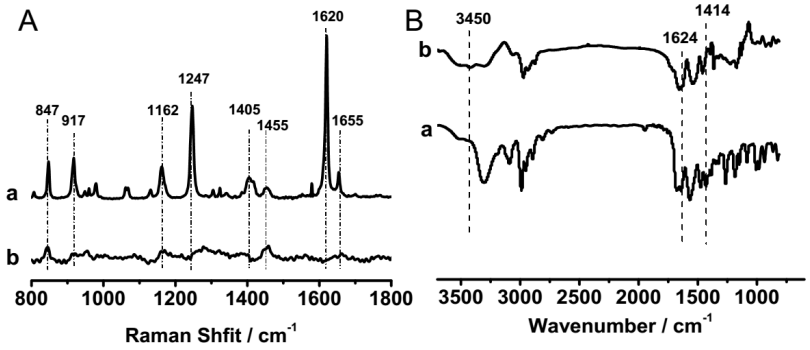

Figure 1. (A) Raman spectra of NIPAAm (a) and PNIPAAm (b); (B) FTIR spectra of NIPAAm (a) and PNIPAAm (b)

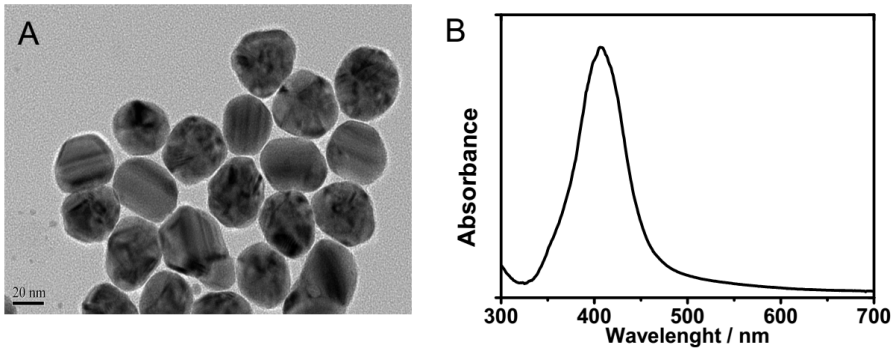

Figure 2. (A) TEM image and (B) UV-vis spectrum of AgNPs.

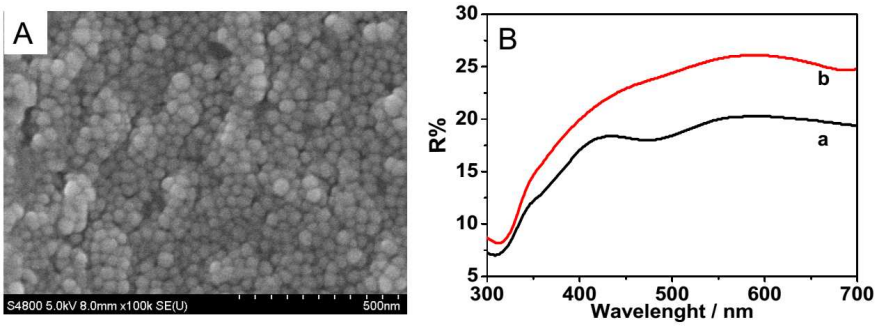

Figure 3. (A) SEM image of PNIPAAm / AgNPs composite film in dry state; (B) UV-reflectance spectra of PNIPAAm/AgNPs composite film at 25 ^{o}C (a) and 40 ^{o}C (b).

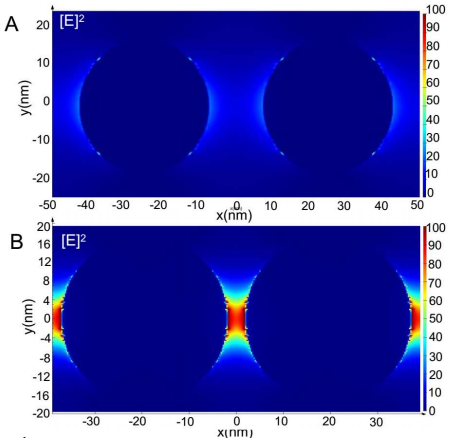

Figure 4. (A) Simulated electric-field profile of PNIPAAm / AgNPs composite film at 25 ^{o}C and (B) 40 ^{o}C.

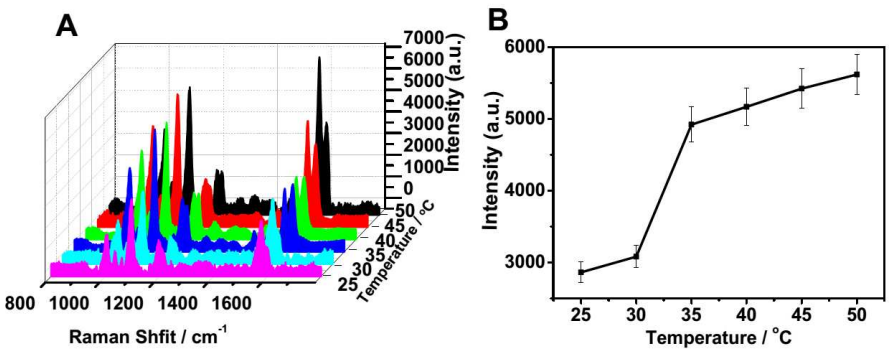

Figure 5. (A) SERS spectra of 1×10^{-4} M 4-Mpy using PNIPAAm / AgNPs composite film as SERS substrate with increasing temperatures and (B) the corresponding temperature-dependent SERS intensity at 1097 cm^{-1} .

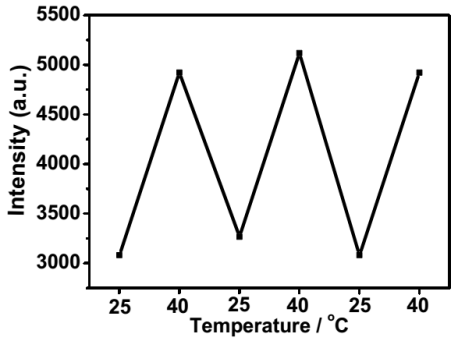

Figure 6. SERS intensity of 4-Mpy at 1097 cm^{-1} during repeated heating (40 ^{o}C) / cooling (25 ^{o}C) cycles.

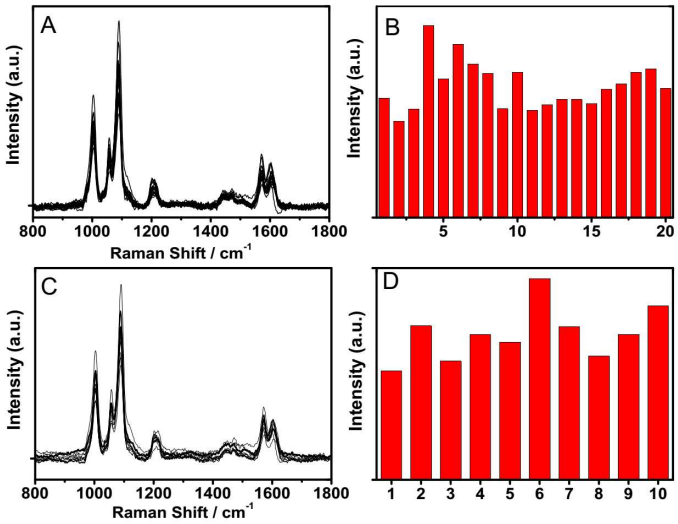

Figure 7. (A) SERS spectra of 4-Mpy (1×10^{-4}M) using PNIPAAm / AgNPs composite film as SERS substrate from 20 randomly selected spots. (B) The intensities of peak (1097 cm^{-1}) at 20 spots on the same substrate. (C) SERS spectra of 4-Mpy (1×10^{-4}M) using different PNIPAAm / AgNPs composite film as SERS substrates. (D) The intensities of peak (1097 cm^{-1}) at different substrate.

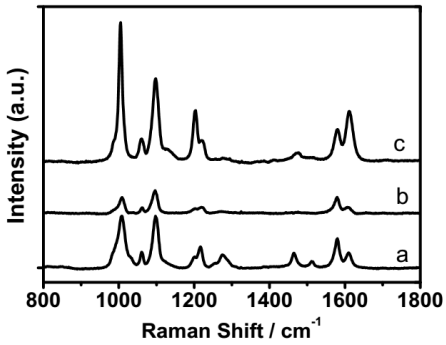

Figure 8. The SERS spectra of 1×10^{-4} M 4-Mpy using PNIPAAm / AgNPs composite film as SERS substrate in H_2O (a), EtOH (b) and EtOH / H_2O mixture (volume ratio = 5:5) (c).